Available online at www.easd.procedia.org
EASD Procedia EURODYN (2026) 1610-1620

EASD Procedia

EURODYN 2026
XIII International Conference on Structural Dynamics
M. Beer, C. Papadimitriou, H. Jensen, J. Chen, M. Broggi, J. Behrensdorf (eds.)
Hannover, Germany, 27.09.–01.10 2026

TIDAL EFFECTS ON MODAL PARAMETERS OF A PILE-SUPPORTED CONCRETE QUAY USING OPERATIONAL MODAL ANALYSIS

Girmay Godifey Wubneh[1], Torodd Skjerve Nord[1], Bernt Johan Leira[2], Aksel Fenerci[3,4], and Bartosz Siedziako[1]

[1]Department of Ocean Operations and Civil Engineering, NTNU, Ålesund, Norway
e-mail: {girmay.g.wubneh, torodd.nord, bartosz.siedziako}@ntnu.no

[2]Department of Marine Technology, Norwegian University of Science and Technology (NTNU), Norway
e-mail: bernt.leira@ntnu.no

[3]Multiconsult, Oslo, Norway
[4]Department of Structural Engineering, NTNU, Norway
e-mail: aksel.fenerci@multiconsult.no

Keywords: operational modal analysis, tidal variation, pile-supported quay, added mass, structural health monitoring

Abstract. *This paper investigates the influence of tidal water level fluctuation on the modal parameters of a pile-supported concrete ferry quay on the Norwegian coast. Ambient vibration data collected continuously over a 24-hour tidal cycle (range: 2.093 m), excluding ferry docking periods, from 16 accelerometers are analysed using covariance-driven stochastic subspace identification applied to 10-minute windows. Five dominant vibration modes are identified in the 0.5–10 Hz range. The fundamental mode (lateral sway) at approximately 2.74 Hz shows a significant negative correlation with water level ($r = -0.76$, $p < 0.001$), with a sensitivity of -0.074 Hz/m, consistent with hydrodynamic added mass effects on the submerged piles. Damping of the first mode increases with water level ($r = 0.52$, $p < 0.001$), indicating that fluid-structure interaction contributes to energy dissipation. Modes 2–5 (second lateral, coupled lateral-longitudinal, and higher-order bending modes) show no statistically significant correlation with water level. The added mass ratio estimated from the frequency shift increases approximately linearly from 2% at low tide to 15–19% at high tide. The observed tidal variability of up to 5.5% of the mean frequency has direct implications for vibration-based structural health monitoring of marine structures.*

ISSN:2311-9020 © 2026 The Authors. Published by EASD Procedia.
Peer-review under responsibility of the Organizing Committee of EURODYN 2026.
doi: 10.47964/1326.10769.319

1 INTRODUCTION

Ferry quays are critical components of coastal transportation infrastructure in Norway, serving more than 40 million passengers and 23 million vehicles annually [1]. These structures are exposed to continuously varying environmental and operational conditions, including tidal fluctuations, wave action, wind, and transient impact forces associated with vessel docking. Despite their societal importance, the dynamic behavior of the ferry quay under such conditions remains poorly characterized in the literature [2, 3]. In recent years, structural health monitoring (SHM) and Operational modal analysis (OMA) have become established tools for assessing the dynamic behavior of civil infrastructure, including bridges, buildings, and offshore structures [4–7]. OMA enables the identification of modal parameters such as natural frequencies, damping ratios, and mode shapes directly from in-service response measurements without requiring controlled excitation. This is particularly advantageous for marine structures that are continuously subjected to environmental loading, and artificial excitation is impractical.

However, modal parameters identified through OMA are known to vary not only due to structural deterioration but also in response to changing environmental and operational conditions [8–10]. Temperature effects on natural frequencies have been extensively studied for bridges [11, 12], and the influence of wind and wave has been documented for long-span structures [13]. Distinguishing between modal variability caused by such benign environmental factors and that caused by genuine structural damage remains an important research problem in vibration-based monitoring.

Among the relevant environmental factors, the influence of water level on the dynamic properties of marine structures has received comparatively little attention. In a laboratory setting, [14] conducted wave flume experiments on a scaled offshore model and demonstrated that natural frequencies decrease with increasing water level due to hydrodynamic added mass, and at the same time acknowledging that damping is an uncertain parameter. Additionally, [14] reported that mode shapes exhibit notable complexity, likely attributable to nonlinearities in the model rather than to water effects.

At full-scale structures, [13] investigated tidal effects on the Bergsøysund floating pontoon bridge and found that tidal level changes have insignificant effects on modal parameters. This result is physically expected, since a floating bridge rises and falls with the tide, maintaining a constant relative water-to-structure geometry. In contrast, fixed pile-supported structures such as ferry quays experience genuine changes in boundary conditions as the water level varies. Tidal fluctuations alter the submerged pile length, affecting hydrodynamic added mass and potentially other fluid–structure interaction mechanisms. These effects are expected to produce measurable changes in modal parameters, yet full-scale evidence quantifying this relationship for pile-supported concrete quay structures remains limited.

The present study investigates the influence of tidal water level variations on the dynamic characteristics of a pile-supported concrete ferry quay equipped with a permanent monitoring system. Continuous vibration data recorded over a full 24-hour tidal cycle at the Magerholm research quay (MRQ) instrumented since 2023 are analyzed using OMA. The identified modal parameters are then compared with corresponding water level measurements obtained from Kartverket [15] to examine the relationship between tidal variations and structural dynamic behavior.

2 THEORETICAL BACKGROUND

2.1 Covariance-driven stochastic subspace identification

The covariance-driven stochastic subspace identification (cov-SSI) method is a time-domain OMA technique that estimates state-space models from output-only response data, and has been shown to be among the most robust techniques for modal identification of civil structures [5, 16–18]. Output correlation matrices are assembled into a block Hankel matrix, whose SVD yields the extended observability matrix. Eigendecomposition of the extracted system matrix $\mathbf{A}$ gives discrete eigenvalues $\hat{\lambda}_r$, from which modal parameters are recovered as:

$$f_r = \frac{|\operatorname{Im}(\ln \hat{\lambda}_r)|}{2\pi\,\Delta t}, \qquad \xi_r = \frac{-\operatorname{Re}(\ln \hat{\lambda}_r)}{|\ln \hat{\lambda}_r|}, \tag{1}$$

$$\boldsymbol{\phi}_r = \mathbf{C}\boldsymbol{\psi}_r, \tag{2}$$

where f_r is the natural frequency, ξ_r the damping ratio, and $\boldsymbol{\phi}_r$ the mode shape for mode r.

2.2 Stabilisation and mode validation

Physical modes are distinguished from spurious poles by requiring stability across consecutive model orders in frequency (ϵ_f), damping (ϵ_ξ), and mode shape similarity quantified by the Modal Assurance Criterion (MAC) [19].

$$\mathrm{MAC}(\boldsymbol{\phi}_a, \boldsymbol{\phi}_b) = \frac{\left|\boldsymbol{\phi}_a^H \boldsymbol{\phi}_b\right|^2}{(\boldsymbol{\phi}_a^H \boldsymbol{\phi}_a)(\boldsymbol{\phi}_b^H \boldsymbol{\phi}_b)} \tag{3}$$

2.3 Added Mass Estimation

For a structure partially submerged in water, the natural frequency is modified by the hydrodynamic added mass. For a single degree of freedom system, the natural frequency with and without added mass are:

$$f = \frac{1}{2\pi}\sqrt{\frac{k}{m + m_a}}, \qquad f_{\mathrm{ref}} = \frac{1}{2\pi}\sqrt{\frac{k}{m}}, \tag{4}$$

where k is the structural stiffness, m the structural modal mass, and m_a the hydrodynamic added mass. Here f_{ref} denotes the reference frequency at the lowest observed water level, where added mass is assumed minimal. The added mass ratio is then estimated directly from the measured frequency shift as:

$$\frac{m_a}{m} = \left(\frac{f_{\mathrm{ref}}}{f}\right)^2 - 1 \tag{5}$$

If the dry modal mass m is known from a finite element model, the absolute added mass follows as $m_a = m\left[(f_{\mathrm{ref}}/f)^2 - 1\right]$.

3 STRUCTURE AND MONITORING SYSTEM

3.1 Description of the Magerholm ferry quay

The Magerholm ferry quay in Møre og Romsdal county on the western Norwegian coast, consists of a pile-supported reinforced concrete deck constructed in 1997 and extended in 2015 to a total length of 100 m. The deck is supported by 23 concrete-filled steel piles, including

several inclined piles providing lateral stiffness. The present study focuses exclusively on the pile-supported deck, excluding the link span that has been extensively studied in [2, 20, 21]. The dominant structural response is expected in the transverse (berthing) direction, governed by lateral deformation of the piles.

3.2 Instrumentation and measurement configuration

The quay has been instrumented with triaxial and uniaxial IEPE accelerometers connected to a National Instruments CompactRIO data acquisition system sampling at 512 Hz since September 2023. The present study uses 16 of the 21 installed channels, distributed across 9 positions on the concrete deck as illustrated in Figure 1, with the majority oriented in the transverse direction to capture the dominant lateral response. The system records continuously, capturing ambient vibrations and approximately 55 daily ferry berthing events.

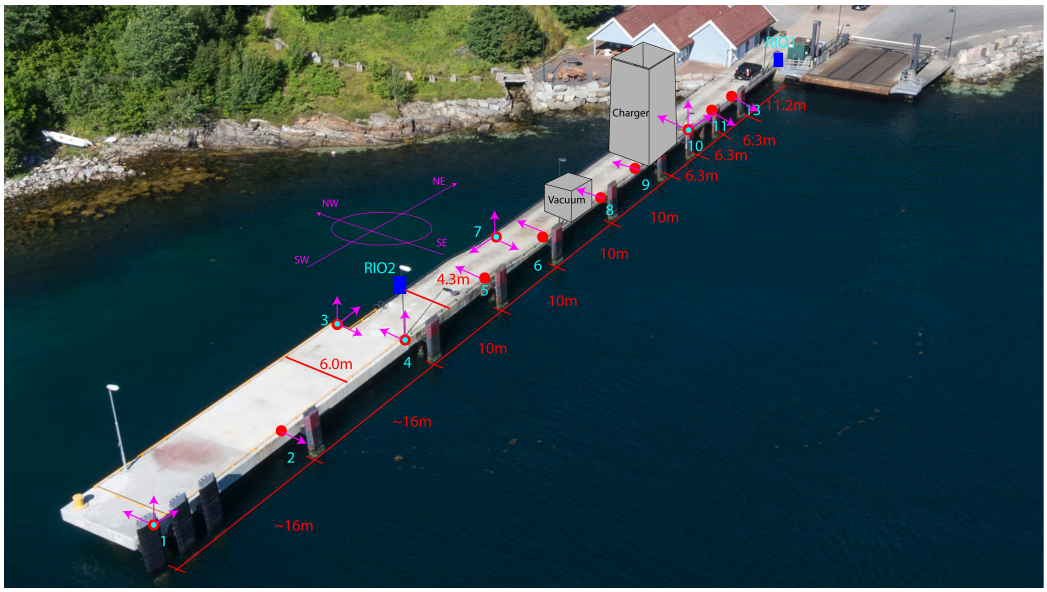


Figure 1: Instrumentation layout of the Magerholm ferry quay showing accelerometer locations and measurement directions on the concrete deck.

4 METHODOLOGY

4.1 Data processing pipeline

Data are recorded continuously in hourly TDMS files (512 Hz, 16 channels). Each hourly file is processed as follows:

1. **Window extraction:** Three 10-minute segments are extracted per hour at minutes 10–20, 30–40, and 50–60, avoiding intervening segments likely dominated by ferry docking events.

2. **Preprocessing:** Voltage signals are converted to acceleration (m/s^2), resampled from 512 Hz to 128 Hz, linearly detrended, and bandpass filtered using a 4th-order Butterworth filter (0.5–20 Hz).

3. **Cov-SSI and stabilisation:** Modal identification is performed on each window using the parameters in Table 1, and stable poles are clustered into physical modes.

4. **Mode tracking:** Modes are tracked across all windows using combined MAC and frequency proximity criteria.

This yields 72 modal parameter estimates per day (3 windows × 24 hours), each associated with a water level value interpolated from the 10-minute tide gauge data.

Parameter	Value
Sampling rate (resampled)	128 Hz
Window duration	10 min (76 800 samples)
Block rows (i)	150
Maximum time lag ($\tau_{\max}$)	2.34 s
Model orders	10, 12, . . . , 100
Frequency stability (ϵ_f)	1%
Damping stability (ϵ_ξ)	5%
MAC stability (ϵ_{MAC})	0.95
Minimum stable count	8
Frequency band of interest	0.5–20 Hz
Damping bounds	0.1%–20%

Table 1: Cov-SSI analysis parameters.

5 RESULTS

5.1 Identified modes

Five vibration modes were consistently identified in the frequency range 0.5–10 Hz (Table 2). Figure 2 shows a representative stabilisation diagram for a single 10-minute window, illustrating the clear vertical alignment of stable poles at the five identified modal frequencies.

Mode	Mode description	Mean freq. (Hz)	Std (Hz)	Mean damp. (%)	Std (%)	N
1	Lateral sway	2.74	0.0706	4.51	1.92	59
2	Second lateral	3.62	0.1284	3.13	1.39	47
3	Coupled lat.–long.	5.47	0.0772	2.42	0.81	26
4	Lateral bending	6.61	0.0912	2.48	0.41	37
5	Torsional	7.51	0.178	3.24	1.29	19

Table 2: Summary of identified modal parameters from 24-hour analysis (72 windows). N indicates the number of windows where the mode was successfully identified.

The fundamental mode (Mode 1, ∼ 2.74 Hz) was identified in 82% of all windows, providing the most robust dataset for statistical analysis and is therefore selected for further investigation of tidal water-level effects and added-mass ratio estimation.

5.2 Tidal influence on natural frequencies

During the 24-hour monitoring period, the tidal range was 2.093 m, with water levels varying from −0.896 m to +1.197 m. Figure 3 shows the temporal variation of the fundamental frequency

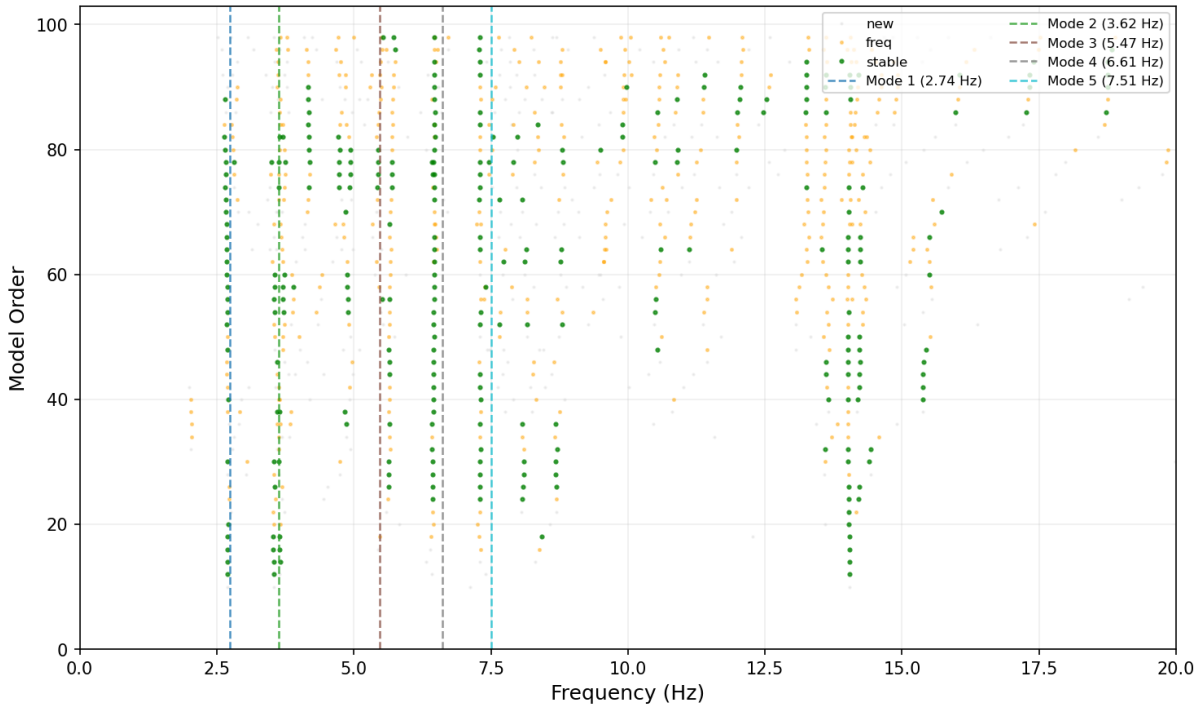


Figure 2: Representative stabilisation diagram. Stable poles are shown in green; dashed lines indicate modal frequencies.

f_1 alongside the measured water level over the 24-hour monitoring period. A clear anti-phase relationship is visible: f_1 decreases during rising tide and recovers during falling tide, with two complete tidal cycles producing corresponding frequency oscillations. This visual pattern motivates the statistical analysis that follows. Table 3 presents the Pearson correlation coefficients and linear sensitivities between modal parameters and water level.

			Frequency–water level			Damping–water level		
Mode	Mean freq. (Hz)	N	r	p	Hz/m	r	p	%/m
1	2.74	59	−0.76	<0.001*	−0.074	0.52	<0.001*	1.38
2	3.64	47	−0.08	0.611	−0.015	−0.01	0.958	−0.02
3	5.54	26	−0.24	0.248	−0.027	−0.29	0.144	−0.35
4	6.53	37	−0.26	0.117	−0.035	0.21	0.220	0.13
5	7.50	19	0.00	0.989	0.001	−0.22	0.370	−0.38

Table 3: Correlation between modal parameters and water level. Significance levels: * $p < 0.05$. Results not statistically significant ($p > 0.05$) are shown in gray.

Mode 1 shows a statistically significant negative correlation between frequency and water level ($r = -0.76$, $p < 0.001$), with a sensitivity of −0.074 Hz/m, consistent with the hydrodynamic added-mass effect: as the water level rises, more pile length is submerged, increasing the effective vibrating mass and reducing the natural frequency. Higher modes (2–5) show no statistically significant frequency–water level correlation (all $p > 0.05$, Table 3). The insensitivity of higher modes to tidal variation is likely attributable to three factors: (i) higher modes are likely to have

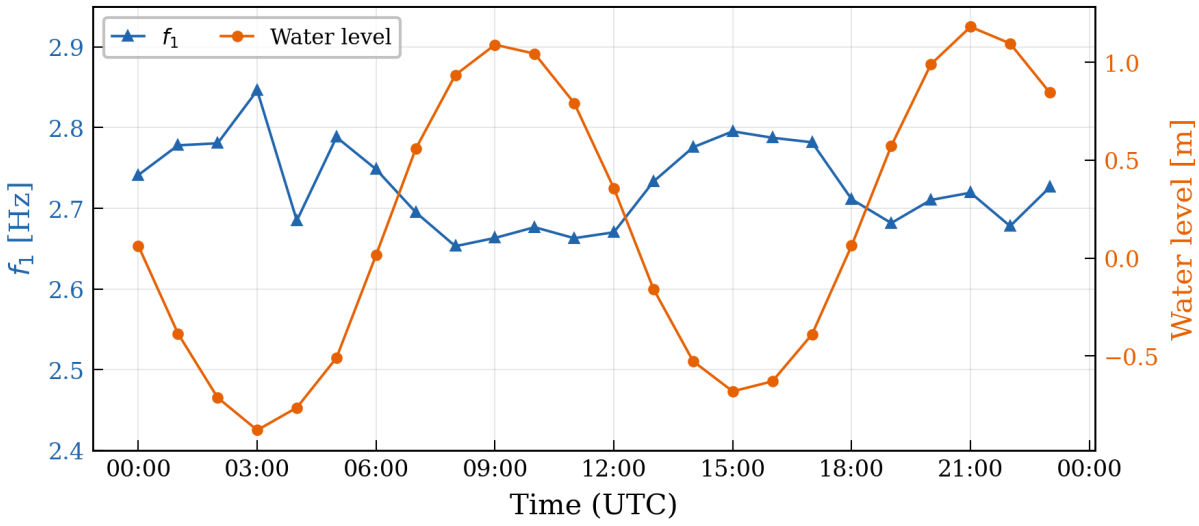


Figure 3: Temporal variation of Mode 1 natural frequency and tidal water level over the 24-hour monitoring period.

node locations near piles, reducing direct pile involvement, (ii) modes 2–5 are dominated by deck bending and torsional motion with limited engagement of the submerged pile structure, and (iii) the effective added mass contribution from the submerged portion is small. This contrasts with [13], who reported insignificant tidal effects on a floating pontoon bridge, confirming that tidal sensitivity is structure-type dependent.

Mode 1 also exhibits a significant positive damping–water level correlation ($r = 0.52$, $p < 0.001$, sensitivity +1.38 %/m), indicating that increased viscous dissipation from the expanding wetted surface area of the piles contributes meaningfully to energy loss at higher water levels. No significant damping–water level correlations were found for higher modes, consistent with [14], who noted that damping estimates exhibit considerably more scatter than frequency estimates.

The resulting tidal frequency variability of approximately 5.5% of the mean, must be accounted for in high-fidelity models and in vibration-based SHM schemes, so that frequency drops caused by tidal variation are not misinterpreted as structural degradation and do not trigger false alarms.

5.3 Mode shapes under tidal extremes

Figure 4 compares the Argand diagrams of the five identified modes at high and low tide. The mode shape vectors remain qualitatively stable between tidal states, with consistent directional dominance (lateral for Modes 1–2, coupled lateral–longitudinal for Mode 3, lateral-bending for Mode 4 and torsional for Mode 5). This indicates that tidal variation primarily affects the natural frequencies and damping ratios rather than the mode shapes themselves. Note that higher mode shape estimates should be interpreted with caution given the sparse spatial distribution of measurement points on the deck. The most notable difference is the Mode 1 damping ratio, which increases from 3.6 % at low tide to 5.8 % at high tide, consistent with enhanced hydrodynamic damping at greater submersion depth. The corresponding frequency shift (2.82 to 2.68 Hz) reflects the added-mass effect discussed in the above section.

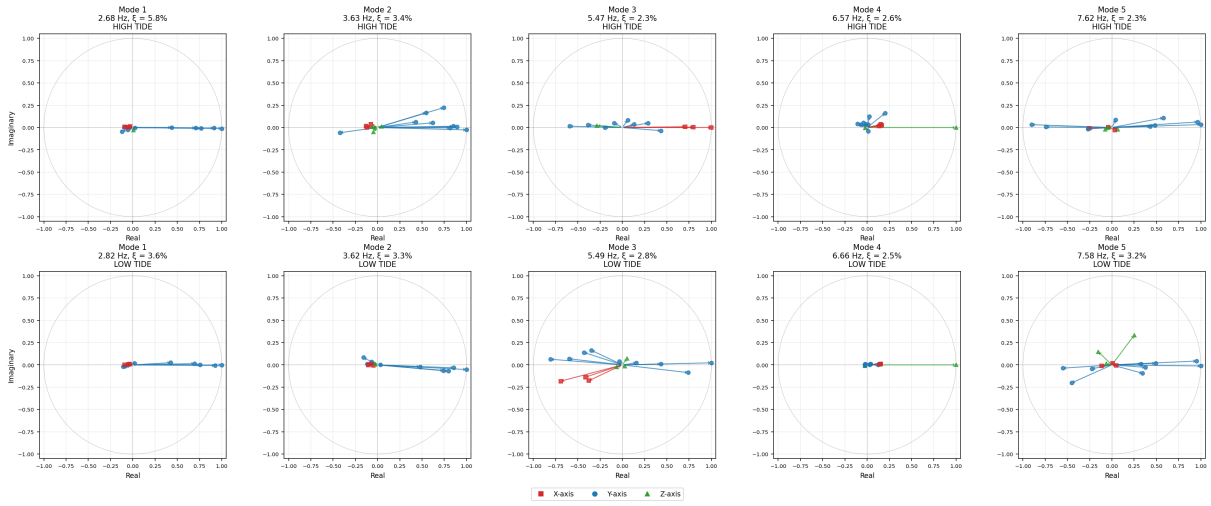


Figure 4: Argand diagrams of the five identified modes at high tide (top) and low tide (bottom). Modal components shown for X-direction (red squares), Y-direction (blue circles), and Z-direction (green triangles).

5.4 Added mass ratio estimation

The observed frequency–water level relationship can be interpreted through the added mass concept. Assuming the structural stiffness remains constant and only the effective mass changes with water level, the added mass ratio for each window is estimated as:

$$\frac{m_a}{m_{\text{eff}}} = \left(\frac{f_{\text{ref}}}{f_i}\right)^2 - 1 \tag{6}$$

where f_{ref} is the reference frequency at the lowest observed water level and f_i is the frequency measured in window i.

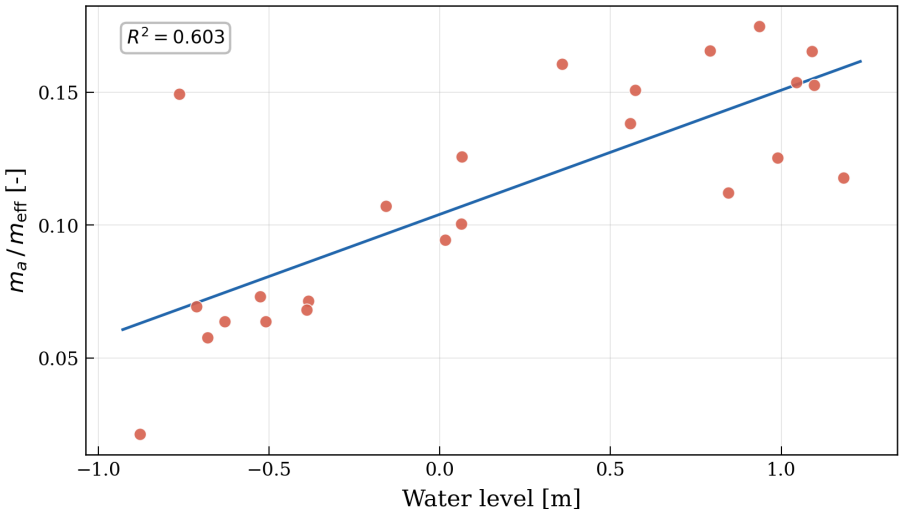


Figure 5: Hourly averaged added mass ratio m_a/m_{eff} versus mean water level for Mode 1. Linear regression: $R^2 = 0.603$.

Equation (6) is used as a practical modal-level proxy for added mass. A more rigorous estimate would require FE-based modal mass normalization and possibly Morison-type hydrodynamic

modelling, particularly given that a pile-supported quay is a multi-degree-of-freedom system. This refinement is planned for future work. Figure 5 shows the hourly averaged added mass ratio as a function of mean water level. The linear relationship ($R^2 = 0.603$) demonstrates a strong quantifiable correlation between water level and added mass. The ratio increases approximately linearly from about 2% at the lowest tide to 15–19% at the highest tide, confirming that a substantial fraction of the effective vibrating mass is of hydrodynamic origin. Although tidal level is the dominant factor, other parameters such as currents, wave conditions, and deck temperature may contribute to the residual scatter and will be considered in extended multi-month analyses.

6 CONCLUSIONS

This study presents a systematic investigation of tidal water level effects on the modal parameters of a full-scale pile-supported concrete quay using continuous operational modal analysis. The main conclusions are:

1. The fundamental lateral bending mode at approximately 2.74 Hz exhibits a statistically significant inverse relationship with water level ($r = -0.76$, $p < 0.001$), with a sensitivity of −0.074 Hz/m attributed to hydrodynamic added mass acting on the submerged piles. Mode shapes remain qualitatively stable between tidal extremes, confirming that tidal variation predominantly affects frequency and damping rather than the spatial deformation pattern.

2. Damping of the fundamental mode increases with water level ($r = 0.52$, $p < 0.001$, sensitivity +1.38 %/m), indicating that fluid–structure interaction contributes to significant energy dissipation. Higher modes (2–5) show no statistically significant sensitivity to tidal variation in either frequency or damping.

3. The added mass ratio estimated from the observed frequency shift increases approximately linearly from 2% at low tide to 15–19% at high tide, demonstrating that hydrodynamic mass constitutes a substantial and variable fraction of the effective vibrating mass for pile-supported marine structures.

4. The tidal-induced frequency variability of up to 5.5% of the mean value is comparable in magnitude to shifts that could indicate structural damage. Environmental compensation models used in vibration-based structural health monitoring of pile-supported marine structures should therefore include water level as a covariate alongside temperature to avoid false positive damage alarms.

Future work will extend the monitoring period to seasonal timescales to separate tidal and temperature effects, develop a finite element model for calibration of the added mass estimates, and investigate the influence of ferry docking forces on the identified modal parameters.

ACKNOWLEDGEMENTS

The authors gratefully acknowledge the support from the Research Council of Norway through the SARTORIUS project (Project No. 353029), Møre og Romsdal Fylke for access to ferry quays, and Sigma2 for national e-infrastructure resources. The authors also gratefully acknowledge the Norwegian Mapping Authority (Kartverket) for tide-gauge data.

REFERENCES

[1] Statens vegvesen. *Ferjedatabanken: Ferry statistics database*. https://ferjedatabanken.no/statistikk. Accessed: 15 March 2026. 2025.

[2] Luigi Sibille et al. "Characterization and analysis of ferry impacts on the Magerholm ferry quay". In: *Measurement* (2025), p. 118551.

[3] Bartosz Siedziako, Torodd Nord, and Luigi Sibille. "The potential of applying structural health monitoring to ferry docks bridges in Norway". In: *IABSE Congress San Jose 2024: Beyond Structural Engineering in a Changing World* (2024). DOI: 10.2749/sanjose.2024.0771.

[4] Charles R Farrar and Keith Worden. *Structural health monitoring: a machine learning perspective*. John Wiley & Sons, 2012.

[5] Bart Peeters and Guido De Roeck. "Stochastic system identification for operational modal analysis: a review". In: *Journal of Dynamic Systems, Measurement, and Control* 123.4 (2001), pp. 659–667.

[6] Vahid Reza Gharehbaghi et al. "A critical review on structural health monitoring: Definitions, methods, and perspectives". In: *Archives of computational methods in engineering* 29.4 (2022), pp. 2209–2235.

[7] Rune Brincker and Carlos Ventura. *Introduction to operational modal analysis*. John Wiley & Sons, 2015.

[8] Hoon Sohn. "Effects of environmental and operational variability on structural health monitoring". In: *Philosophical Transactions of the Royal Society A: Mathematical, Physical and Engineering Sciences* 365.1851 (2007), pp. 539–560.

[9] A-M Yan et al. "Structural damage diagnosis under varying environmental conditions—Part I: A linear analysis". In: *Mechanical Systems and Signal Processing* 19.4 (2005), pp. 847–864.

[10] A-M Yan et al. "Structural damage diagnosis under varying environmental conditions—part II: local PCA for non-linear cases". In: *Mechanical Systems and Signal Processing* 19.4 (2005), pp. 865–880.

[11] Bart Peeters and Guido De Roeck. "One-year monitoring of the Z24-Bridge: environmental effects versus damage events". In: *Earthquake engineering & structural dynamics* 30.2 (2001), pp. 149–171.

[12] Filipe Magalhães, Álvaro Cunha, and Elsa Caetano. "Dynamic monitoring of a long span arch bridge". In: *Engineering Structures* 30.11 (2008), pp. 3034–3044.

[13] Knut Andreas Kvåle, Ole Øiseth, and Anders Rønnquist. "Operational modal analysis of an end-supported pontoon bridge". In: *Engineering Structures* 148 (2017), pp. 410–423.

[14] Michael Vigsø et al. "Operational modal analysis and fluid-structure interaction". In: *28th International Conference on Noise and Vibration Engineering (ISMA 2018)*. 2018.

[15] Norwegian Mapping Authority (Kartverket). *Sea level and tide observations for Ålesund*. Accessed: 2025-12-18. 2024. URL: https://www.kartverket.no/en.

[16] Edwin Reynders. "System identification methods for (operational) modal analysis: review and comparison". In: *Archives of computational methods in engineering* 19.1 (2012), pp. 51–124.

[17] Luc Hermans and Herman Van der Auweraer. “Modal testing and analysis of structures under operational conditions: industrial applications”. In: *Mechanical systems and signal processing* 13.2 (1999), pp. 193–216.

[18] Edwin Reynders et al. “Uncertainty quantification in operational modal analysis with stochastic subspace identification: Validation and applications”. In: *Mechanical Systems and Signal Processing* 66 (2016), pp. 13–30.

[19] Randall J Allemang. “The modal assurance criterion–twenty years of use and abuse”. In: *Sound and vibration* 37.8 (2003), pp. 14–23.

[20] Luigi Sibille et al. “Structural Health Monitoring of a Ferry Quay: Instrumentation and Impact of Tidal Levels on Modal Parameters”. In: *Structural Health Monitoring & Machine Learning, Vol. 12*. River Publishers, 2026, pp. 23–31.

[21] Luigi Sibille. “Structural Health Monitoring and Digital Twin Approaches for the Dynamic Assessment of Ferry Quays”. PhD thesis. Trondheim, Norway: Norwegian University of Science and Technology (NTNU), 2026. URL: https://hdl.handle.net/11250/5341829.